

SAGE3D: SOFT-GUIDED ATTENTION AND GRAPH EXCITATION FOR 3D POINT CLOUD CORNER DETECTION

Batuhan Arda Bekar*

Can Sari*

Hüseyin Can Gülkan*

Barış Özcan*

* Bahçeşehir University
Computer Engineering

{batuhanarda.bekar, can.sari, huseyin.gulkan}@bahcesehir.edu.tr,
baris.ozcan@bau.edu.tr

ABSTRACT

We present SAGE3D, a hybrid Transformer-based model for corner detection in airborne LiDAR point clouds. We propose a multi-stage solution built on a hierarchical encoder-decoder architecture that progressively downsamples point clouds through Set Abstraction layers and recovers per-point predictions via Feature Propagation. We introduce two innovations: Soft-Guided Attention, which injects ground-truth corner labels as a log-prior into attention logits during training to improve precision; then an Excitatory Graph Neural Network positioned at strategic resolutions in the hierarchy, employing positive-only message passing where high-confidence corners reinforce predictions through learned boosting, optimizing for recall. The hierarchical design enables multi-scale feature extraction while our guided attention and excitatory modules ensure corner signals are amplified rather than diluted across scales.

Index Terms— 3d point clouds, corner detection, graph neural network

1. INTRODUCTION

The automatic reconstruction of 3D building models from airborne LiDAR point clouds is a fundamental task in urban scene understanding, with applications spanning smart cities [1], digital twin generation, and autonomous driving [2]. Accurate corner detection is the critical prerequisite for wireframe reconstruction, yet it faces unique challenges compared to 2D image analysis.

The primary difficulty is extreme class imbalance: corners typically constitute less than 1% of points, with the vast majority belonging to planar surfaces. Furthermore, point clouds lack the regular grid structure of images, requiring specialized architectures that can reason about local geometry while maintaining global context.

Recent advances in point cloud processing have established hierarchical architectures as the dominant paradigm. PointNet++ [3] introduced Set Abstraction layers that progressively downsample points while aggregating local fea-

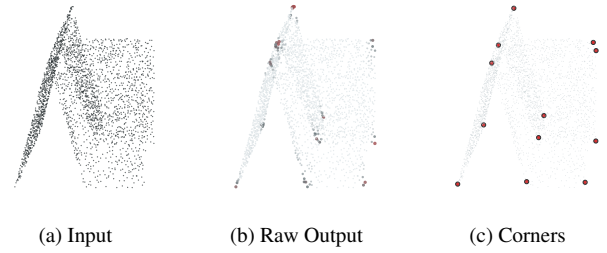


Fig. 1. SAGE3D pipeline. (a) Raw LiDAR input. (b) Per-point corner probabilities (gray→red). (c) Final corners after DBSCAN.

tures, followed by Feature Propagation for per-point predictions. Point Transformer [4] extended this with vector attention mechanisms that capture fine-grained geometric relationships. However, these methods treat all points equally during feature learning, which is suboptimal when the task exhibits severe class imbalance.

Graph Neural Networks (GNNs) offer a complementary approach by enabling message passing between points based on spatial proximity [5]. Traditional message passing may tend to over-smooth features, suppressing isolated corner signals in favor of their predominantly non-corner neighbors.

In this paper, we propose SAGE3D, a hybrid architecture that addresses these challenges through two key innovations. First, we introduce *Soft-Guided Attention*, inspired by teacher forcing [6] and privileged information learning [7], which leverages ground-truth corner proximity during training to bias transformer attention toward geometrically salient regions. Second, we propose an *Excitatory Graph Neural Network*, inspired by Graph Attention Networks [8], where high-confidence corners boost neighboring predictions through strictly positive message passing. Our contributions are: (1) Soft-Guided Attention that injects ground-truth corner proximity as a differentiable log-prior; (2) an Excitatory GNN with positive-only message passing; and (3) 4D position encodings augmenting relative coordinates with Euclidean distance.

2. METHODOLOGY

Inspired by Point2Roof [9], our encoder-decoder architecture processes raw point clouds to detect wireframe corners. The encoder hierarchically abstracts features through four Set Abstraction (SA) layers, while the decoder restores point-wise predictions via Feature Propagation (FP) layers with skip connections. Input point clouds contain 8 channels: normalized XYZ coordinates (3), RGBA color and intensity (5). We first randomly subsample 2560 points from the original point cloud, and enter the encoder.

2.1. Encoder: Set Abstraction

Each SA layer downsamples points and aggregates local features. SA1–SA3 use multi-scale grouping with Point Transformer blocks, while SA4 uses single-scale grouping with Soft-Guided Attention. CentroidGNN modules are applied after SA2 and SA4 to amplify corner-related features.

Downsampling. FPS selects representative subsets at each layer, progressively reducing points via 4x, 2x, 2x, 4x downsampling from 2560 to 40 points through the four SA layers.

Point Transformer with 4D Position Encoding. Each Point Transformer block aggregates neighbor information using vector attention [10]. Given center point i with features f_i and coordinates \mathbf{p}_i , we use k -NN to gather the K nearest neighbors ($K \in \{16, 32\}$). We compute 4D position encodings:

$$\delta_j = \theta([\mathbf{p}_i - \mathbf{p}_j, \|\mathbf{p}_i - \mathbf{p}_j\|]) \quad (1)$$

where θ is a two-layer MLP. Vector attention computes weights through element-wise subtraction:

$$\mathbf{w}_j = \phi(\mathbf{q}_i - \mathbf{k}_j + \delta_j), \tilde{f}_i = \sum_j \text{softmax}(\mathbf{w}_j) \odot (\mathbf{v}_j + \delta_j) \quad (2)$$

where $\mathbf{q}, \mathbf{k}, \mathbf{v}$ are linear projections and ϕ is an MLP.

Soft-Guided Attention. At SA4, we bias attention toward likely corners by adding a log-prior to attention logits:

$$\mathbf{w}'_j = \mathbf{w}_j + \log(y_j + \epsilon) \quad (3)$$

where $y_j \in [0, 1]$ are soft labels computed from ground truth during training, and $\epsilon = 0.01$. Following the Learning Using Privileged Information (LUPI) paradigm [7], this log-prior acts purely as a training signal to shape the learned attention weights. At inference, where there exists no ground truth data, the guidance is removed and we utilize the identical Vector Attention mechanism shown in Equation (2).

CentroidGNN: Excitatory Message Passing. CentroidGNN applies excitatory-only message passing after SA2 and SA4. Unlike standard GNNs that can suppress features, our design only amplifies:

$$f'_i = f_i + \sigma(\alpha) \cdot \psi \left(\sum_{j \in \mathcal{N}(i)} \tilde{a}_{ij} \cdot m_{ij} \right) \quad (4)$$

where $m_{ij} = \text{ReLU}(\text{MLP}([f_i, f_j, d_{ij}]))$ are positive-only messages, $\tilde{a}_{ij} = a_{ij} \cdot (1 + c_i \cdot c_j)$ are attention weights boosted by corner-to-corner affinity, ψ is a learned transform, and $\sigma(\alpha)$ is a sigmoid-gated mixing coefficient.

2.2. Decoder: Feature Propagation

The decoder restores full resolution through four FP layers with U-Net-style skip connections [11]. Each FP layer up-samples features using inverse-distance weighted interpolation from three nearest neighbors [3]:

$$f_i = \frac{\sum_{j=1}^3 w_j \cdot f_j}{\sum_{j=1}^3 w_j}, \quad w_j = \frac{1}{\|\mathbf{p}_i - \mathbf{p}_j\|^2 + \epsilon} \quad (5)$$

2.3. Output Heads

Two parallel heads process the final 128-dimensional features: a classification head (MLP: 128→64→1) producing per-point corner logits, and a regression head (MLP: 128→64→3) predicting 3D offset vectors toward the nearest ground-truth vertex.

3. LOSS DESIGN

Our training objective combines distance-weighted classification and regression losses: $\mathcal{L} = \mathcal{L}_{\text{dist}} + \mathcal{L}_{\text{offset}}$.

Soft Label Generation. We generate soft corner labels based on proximity to ground-truth vertices using exponential decay: $y_i^{\text{cls}} = \exp(-d_i/d_{\text{thresh}})$, where $d_i = \min_j \|\mathbf{p}_i - \mathbf{v}_j\|$ and $d_{\text{thresh}} = 0.05$.

Distance-Weighted Focal Loss. We use focal loss [12] with proximity-based weighting:

$$\mathcal{L}_{\text{dist}} = \frac{1}{N} \sum_i w_i \cdot \alpha(1 - p_t)^\gamma \cdot \text{BCE}(\hat{y}_i, y_i) \quad (6)$$

where $w_i = 1 + \beta \exp(-d_i/d_{\text{thresh}})$ with $\beta = 2.0$, and

$$p_t = \begin{cases} \hat{y}_i & \text{if } y_i = 1 \\ 1 - \hat{y}_i & \text{otherwise} \end{cases} \quad (7)$$

Offset Regression Loss. For points within d_{thresh} of a corner, we supervise offset prediction with Smooth L1 loss, following the design of existing 3D object detection methods [13].

4. POST-PROCESSING AND INFERENCE

At inference, points exceeding confidence threshold $\tau = 0.3$ are selected as corner candidates with offset-refined positions. We apply DBSCAN [14] with $\epsilon = 0.05$ and $\text{minPts} = 1$ to group nearby predictions, then compute cluster centroids as final corners.

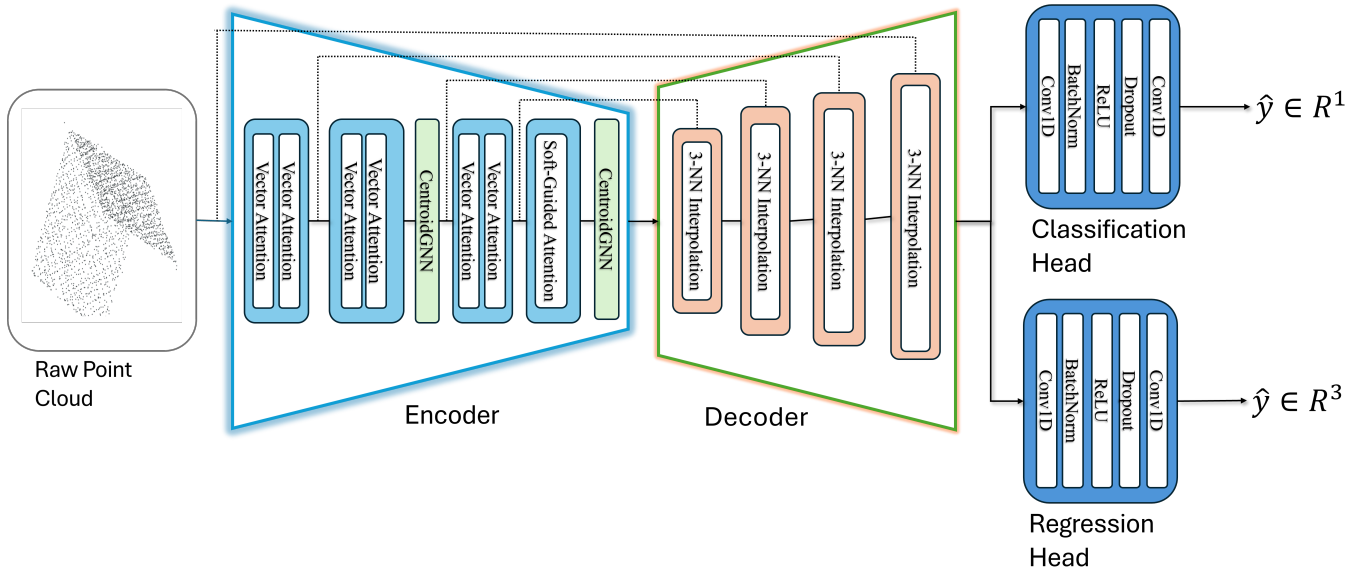


Fig. 2. SAGE3D architecture. The encoder uses four Set Abstraction layers with Point Transformer blocks; CentroidGNN modules at SA2 and SA4 boost corner features. The decoder upsamples via 3-NN interpolation with skip connections.

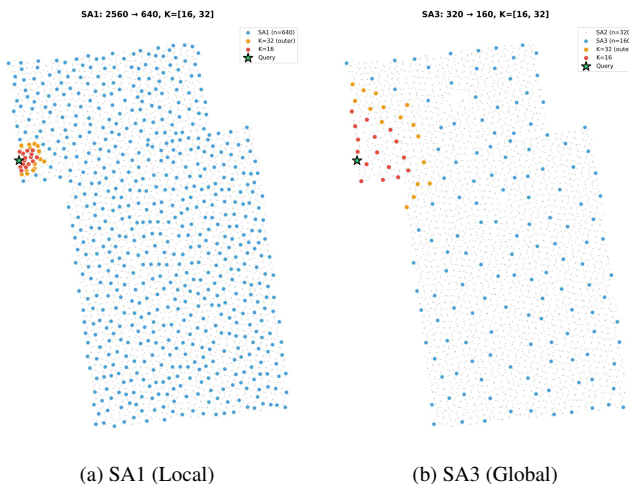


Fig. 3. k -NN grouping at different depths. Same K covers larger spatial extent in deeper layers.

5. EXPERIMENTAL RESULTS

5.1. Implementation Details

The model is implemented in PyTorch and trained on a desktop PC with an RTX 4070 GPU (12GB VRAM), batch size 14. We use AdamW with weight decay 0.01 and OneCycleLR schedule over 60 epochs (max LR 0.01, 10% warmup, cosine annealing). Training takes roughly 1 day on the Building3D Tallinn dataset. We evaluate using Average Corner Offset (ACO), Corner Precision (CP), Corner Recall (CR), and Corner-F1 (CF1) with Hungarian algorithm matching [15].

Table 1. Ablation study on Building3D Entry-Level dataset.

Architecture	CP	CR	F1
PointNet++ (Base)	88.9	68.4	75.98
+ CentroidGNN	87.6	73.3	78.16
+ Point Transformer	84.8	80.6	81.15
+ Soft-Guided Attention	91.5	79.7	83.99

Table 2. Corner detection results on Building3D Tallinn dataset.

Method	ACO \downarrow	CP	CR	CF1
PointMAE*	0.330	75.0	47.0	58.0
PointM2AE*	0.320	79.0	58.0	67.0
Point2Roof [9]	0.390	65.0	30.0	41.0
Supervised [16]	0.290	90.0	53.0	66.0
PBWR [17]	0.222	98.5	68.8	81.0
BWFormer \dagger [18]	0.203	92.5	86.6	89.4
SAGE3D (Ours)	0.134	91.9	74.4	82.2

*Building3D baseline. \dagger From public leaderboard.

5.2. Ablation Study

Table 1 presents an architectural comparison on the Building3D Entry-Level dataset, progressively adding components to evaluate their individual contributions.

5.3. Quantitative Results

Table 2 compares SAGE3D against published methods on the Building3D Tallinn dataset.

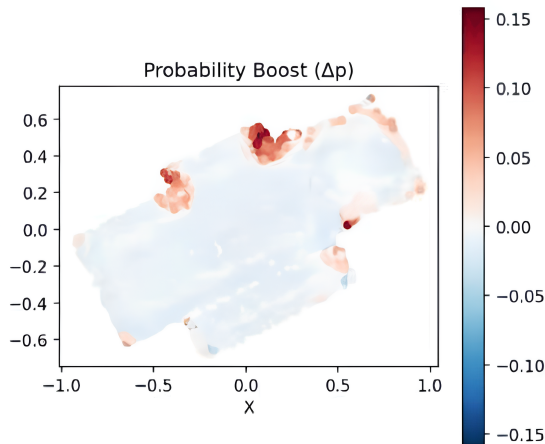


Fig. 4. CentroidGNN probability boost (Δp). Red regions show increased corner confidence after excitatory message passing.

SAGE3D achieves 82.2% CF1 while attaining an ACO of **0.134**, reducing average corner offset by 39.6% compared to PBWR and 34.3% compared to BWFormer. This matters because wireframe quality is highly sensitive to endpoint accuracy: small corner localization errors propagate into incorrect edge endpoints and skewed roof polygons.

Hardware Comparison. PBWR reports training on a single NVIDIA A6000 requiring approximately six days, while BWFormer uses $8 \times$ A800 GPUs for about 1.5 days. Our SAGE3D model trains on a single RTX 4070 in roughly one day, providing highly accurate corner detection while remaining accessible without enterprise-grade infrastructure.

6. CONCLUSION

This paper introduces SAGE3D, a hybrid Transformer and GNN architecture for efficient 3D corner detection. By proposing Soft-Guided Attention to inject geometric priors and an Excitatory GNN to boost recall, we achieve state-of-the-art localization accuracy (0.134 ACO) on the Building3D benchmark using a single consumer-grade GPU. This establishes SAGE3D as a viable solution for resource-constrained environments where deployment efficiency and geometric precision are highly relevant.

7. REFERENCES

- [1] Yuzhou Liu, Lingjie Zhu, Xiaodong Ma, Hanqiao Ye, Xiang Gao, Xianwei Zheng, and Shuhan Shen, “Poly-room: Room-aware transformer for floorplan reconstruction,” in *European Conference on Computer Vision*. Springer, 2024, pp. 322–339.
- [2] Bencheng Liao, Shaoyu Chen, Xinggong Wang, Tianheng Cheng, Qian Zhang, Wenyu Liu, and Chang Huang, “Maptrv2: An end-to-end framework for online vectorized hd map construction,” in *International Journal of Computer Vision*, 2024.
- [3] Charles Ruizhongtai Qi, Li Yi, Hao Su, and Leonidas J Guibas, “Pointnet++: Deep hierarchical feature learning on point sets in a metric space,” *Advances in Neural Information Processing Systems*, vol. 30, 2017.
- [4] Hengshuang Zhao, Li Jiang, Jiaya Jia, Philip HS Torr, and Vladlen Koltun, “Point transformer,” in *IEEE/CVF International Conference on Computer Vision*, 2021, pp. 16259–16268.
- [5] Yue Wang, Yongbin Sun, Ziwei Liu, Sanjay E Sarma, Michael M Bronstein, and Justin M Solomon, “Dynamic graph cnn for learning on point clouds,” *ACM Transactions on Graphics*, vol. 38, no. 5, pp. 1–12, 2019.
- [6] Alex M Lamb, Anirudh Goyal, Ying Zhang, Saizheng Zhang, Aaron C Courville, and Yoshua Bengio, “Professor forcing: A new algorithm for training recurrent networks,” *Advances in Neural Information Processing Systems*, vol. 29, 2016.
- [7] Vladimir Vapnik and Akshay Vashist, “Learning using privileged information: Similarity control and knowledge transfer,” *Journal of Machine Learning Research*, vol. 12, pp. 2023–2049, 2011.
- [8] Petar Velickovic, Guillem Cucurull, Arantxa Casanova, Adriana Romero, Pietro Lio, and Yoshua Bengio, “Graph attention networks,” in *International Conference on Learning Representations*, 2018.
- [9] Li Li, Minhyuk Sung, Anton Duber, and Niloy J Mitra, “Point2roof: End-to-end 3d building roof modeling from airborne lidar point clouds,” *ISPRS Journal of Photogrammetry and Remote Sensing*, vol. 193, pp. 17–28, 2022.
- [10] Xiaoyang Wu, Yixing Lao, Li Jiang, Xihui Liu, and Hengshuang Zhao, “Point transformer v2: Grouped vector attention and partition-based pooling,” in *Advances in Neural Information Processing Systems*, 2022, vol. 35, pp. 33330–33342.

- [11] Olaf Ronneberger, Philipp Fischer, and Thomas Brox, “U-net: Convolutional networks for biomedical image segmentation,” in *Medical Image Computing and Computer-Assisted Intervention*, 2015, pp. 234–241.
- [12] Tsung-Yi Lin, Priya Goyal, Ross Girshick, Kaiming He, and Piotr Dollar, “Focal loss for dense object detection,” *IEEE Transactions on Pattern Analysis and Machine Intelligence*, vol. 42, no. 2, pp. 318–327, 2020.
- [13] Ross Girshick, “Fast R-CNN,” in *IEEE International Conference on Computer Vision*, 2015, pp. 1440–1448.
- [14] Martin Ester, Hans-Peter Kriegel, Jorg Sander, and Xiaowei Xu, “A density-based algorithm for discovering clusters in large spatial databases with noise,” in *International Conference on Knowledge Discovery and Data Mining*, 1996, pp. 226–231.
- [15] Harold W Kuhn, “The hungarian method for the assignment problem,” *Naval Research Logistics Quarterly*, vol. 2, no. 1-2, pp. 83–97, 1955.
- [16] Ruisheng Wang, Jiju Peethambaran, and Dong Chen, “Building3d: An urban-scale dataset and benchmarks for learning roof structures from point clouds,” *IEEE/CVF International Conference on Computer Vision*, pp. 20076–20085, 2023.
- [17] Zhaiyu Huang, Fan Zhang, Zeren Hu, Yao Jin, and Siyan Chen, “Pbwr: Parametric building wireframe reconstruction from aerial lidar point clouds,” *ISPRS Journal of Photogrammetry and Remote Sensing*, vol. 203, pp. 1–14, 2023.
- [18] Yuzhou Liu, Lingjie Zhu, Hanqiao Ye, Shangfeng Huang, Xiang Gao, Xianwei Zheng, and Shuhan Shen, “Bwformer: Building wireframe reconstruction from airborne lidar point cloud with transformer,” in *Proceedings of the Computer Vision and Pattern Recognition Conference*, 2025, pp. 22215–22224.